THE JOURNAL OF PHYSICAL CHEMISTRY B
A JOURNAL OF THE AMERICAN CHEMICAL SOCIETY

pubs.acs.org/JPCB

Article

Zwitterions Layer at but Do Not Screen Electrified Interfaces

Muhammad Ghifari Ridwan, Buddha Ratna Shrestha, Nischal Maharjan, and Himanshu Mishra*

Cite This: J. Phys. Chem. B 2022, 126, 1852−1860

Read Online

ACCESS | Metrics & More | Article Recommendations | Supporting Information

ABSTRACT: The role of ionic electrostatics in colloidal processes is well-understood in natural and applied contexts; however, the electrostatic contribution of zwitterions, known to be present in copious amounts in extremophiles, has not been extensively explored. In response, we studied the effects of glycine as a surrogate zwitterion, ion, and osmolyte on the electrostatic forces between negatively charged mica−mica and silica−silica interfaces. Our results reveal that while zwitterions layer at electrified interfaces and contribute to solutions' osmolality, they do not affect at all the surface potentials, the electrostatic surface forces (magnitude and range), and solutions' ionic conductivity across 0.3−30 mM glycine concentration. We infer that the zwitterionic structure imposes an inseparability among positive and negative charges and that this inseparability prevents the buildup of a counter-charge at interfaces. These elemental experimental results pinpoint how zwitterions enable extremophiles to cope with the osmotic stress without affecting finely tuned electrostatic force balance.

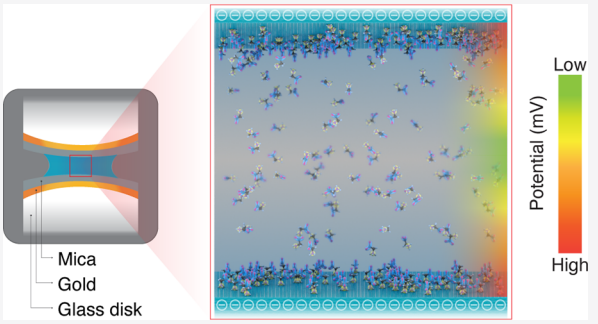

INTRODUCTION

Ions and zwitterions orchestrate the inner workings of prokaryotic, plant, and animal cells via electromagnetic interactions, thereby giving rise to finely tuned structure−function relationships in proteins, chemical reactions, catalysis, molecular recognition and signaling, and bioenergetics.[1−5] Ion electrostatics is also relevant in numerous environmental and industrial contexts, including cloud acidification,[6,7] soil water-holding capacity,[8] microdroplet chemistry,[9−11] stability of pharmaceutical and cosmetic formulations,[12] water desalination[13] and treatment[14] processes, and harvesting nanotriboelectricity.[15] Interestingly, simple hard ions, such as Na^+, K^+, Mg^{2+}, Ca^{2+}, and Cl^-, which are ubiquitous in biological systems, retain their electrical charge irrespective of the solution pH or temperature.[16] Therefore, their presence in excess can tilt the finely tuned balance of molecular forces, notably electrostatics.[2,17−19] The Debye−Hückel model accurately captures the behavior of ions in dilute solution (≲100 mM) on the basis of Maxwell's first law of electromagnetism, $\nabla^2\psi = -\rho/\varepsilon_0\varepsilon_r$, and the assumption that the Boltzmann statistics accurately describes the clustering of the oppositely charged ions at electrified interfaces, $\rho = \rho_0 e^{-e\psi/k_BT}$.[20] This Poisson−Boltzmann equation explains why the clustering of ions dramatically decreases the range and magnitude of electrostatic forces between charges and/or charged surfaces, such as within or among proteins and emulsified oil droplets in water.[21] Such a molecular-scale disruption manifests as cytotoxicity;[22] indeed, salt stress precludes the use of seawater for growing food and forces us to exploit limited and dwindling freshwater resources.[23] This severity echoes in "The Rime of the Ancient Mariner": "Water, water everywhere and not a drop to drink".[24] However, some life forms thrive even in harsh environments, including salty, arid, pressurized, hot, or cold environments, where the amounts of solutes (ions) and solvent (water) can vary dramatically, thereby catastrophically affecting the electrostatics and inducing osmotic imbalance.[1,25,26] The current understanding of how life prevails under such extreme conditions via intermolecular and surface forces is far from satisfactory.[3,27−29]

Osmolytes—electrically neutral molecules such as zwitterionic amino acids (e.g., glycine, proline, and alanine), sugars and polyols (e.g., glucose and glycerol), methylamines (e.g., sarcosine, betaine, and trimethylamineoxide), and urea—orchestrate the balancing act.[1,4,26,30] They are observed in high concentrations in a wide variety of extremophiles, including cyanobacteria, fungi, lichens, multicellular algae, vascular plants, insects, and marine invertebrates and pelagic fishes. Researchers have documented the effects of osmolytes and their compensating effects, such as those of betaine and urea, on enzymatic activities. However, unlike the contributions of hard ions, the contributions of zwitterions to an aquatic solution's ionic strength and surface forces remain unclear. For instance, the zwitterionic contribution to ionic strength has been suggested to

Received: December 7, 2021
Revised: February 7, 2022
Published: February 23, 2022

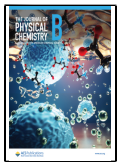

https://doi.org/10.1021/acs.jpcb.1c10388
J. Phys. Chem. B 2022, 126, 1852−1860

be (i) zero,[31] (ii) similar to that of 1:1 salts,[44] and (iii) similar to that of partially charged molecules.[32] Obviously, these proposed contributions would result in drastically different electrostatic forces.[33−35] Therefore, direct measurements of surface forces as a function of surfaces and solutions are necessary to clarify this matter. Recently, Sivan and co-workers used atomic force microscopy (AFM) to probe the effects of adding betaine (1−3 M) on the forces between silica surfaces immersed in solutions comprising NaCl, KCl, CsCl, and $MgCl_2$ at concentrations less than or equal to 50 mM.[36] They found that although the addition of simple ions decreased the range and magnitude of electrostatic forces, betaine (1−3 M) increased both the magnitude and range of electrostatics between silica surfaces. These new results underscore the richness of osmolytes' effects on surface forces and the significance of this research.

Herein, we investigate the effects of glycine as a surrogate osmolyte on electrostatic forces between electrified surfaces at biologically relevant concentrations (<0.6 M) to address the following questions:

1. How do zwitterions influence surface forces between electrically charged surfaces in dilute electrolytes?
(i) Do zwitterions layer at electrified interfaces and screen them similarly to hard ions?
(ii) If zwitterions increase/decrease surface forces, is this effect due to their contribution to the solution's ionic strength or their contribution to its dielectric response?
(iii) If they exert no effect, is the lack of effect attributable to the fortuitous cancellation of their various aforementioned influences?
2. Do zwitterions transition to simple ions if the pH is adjusted to change their charge to, for example, $\pm e$, where e is the electronic charge?
(a) Are the effects of the thus-formed positively and negatively charged ions on surface forces identical?
(b) What is the correlation between the surface forces and the electrolytes' osmotic pressure in these systems?

To probe these nested and interrelated questions, we used AFM and a surface force apparatus (SFA) to measure the forces between electrified silica−silica and mica−mica surfaces separated by dilute aqueous solutions (≤30 mM). The results reveal that zwitterions are much more versatile than hard ions; for instance, they enhance solutions' osmolality but without affecting electrostatic surface forces (magnitude and range).

METHODS

Materials. Glycine, potassium chloride (KCl), potassium hydroxide (KOH), and hydrochloric acid (HCl) were purchased from Sigma-Aldrich and were used as received. Glycine was added to deionized (DI) water from a MilliQ Advantage 10 system (resistivity of 18 MΩ cm, pH 5.7 ± 0.1, and total organic carbon (TOC) ≤ 2 ppm) to prepare solutions with specific concentrations of 0.3, 3, and 30 mM glycine. The solutions were titrated with KOH or HCl to obtain the desired pH. All the experiments were conducted at 21.0 ± 0.5 °C. AFM cantilevers with a silica colloidal tip were purchased from NanoWorld. Si wafers (⟨100⟩ orientation) with a 2.4 μm-thick thermal oxide layer were purchased from Silicon Valley Microelectronics. Muscovite mica substrates were purchased from S&J Trading.

Solution pH, Ionic Conductivity, Osmotic Pressure, and Dielectric Constant. Solutions' pH and conductivity were quantified using a Mettler SevenCompact Duo S213 pH/conductivity benchtop meter. Prior to the measurements, the instrument was calibrated using standard solutions of pH 4, 7, and 10 and solutions with electrical conductivities of 5 μS/cm and 1443 μS/cm. A Vapro 5600 vapor pressure osmometer was used to measure solutions' osmolality after being calibrated with standard solutions with osmolalities of 100, 290, and 1000 mmol/kg. The dielectric constants of solutions were measured using an open-ended coaxial probe connected to a frequency vector analyzer (300 kHz to 4.5 GHz). Prior to the measurement, the instrument was calibrated with open, short, load (DI water) calibration.

Atomic Force Microscopy. A JPK Nanowizard Ultraspeed-II atomic force microscope was used to image glycine adsorbed onto mica surface and measuring the interaction forces between silica surfaces in dilute solutions. For imaging, AFM cantilevers with Sb-doped silica tips (spring constant, k = 2.8 N/m) were used in the tapping mode. For the surface force measurement, AFM cantilevers with silica colloidal probes at their tips (tip diameter, $D = 15 \pm 3$ μm; k = 0.32 N/m) were used against SiO_2 (2.4 μm)/Si wafers with a ⟨001⟩ orientation. The sensitivity and k of the cantilevers were calibrated via the contact-based and thermal noise methods, respectively.[37] The force between the colloidal probe and the substrate was measured by recording the deflection, Δd, which was converted into force using Hooke's law, $F = k\Delta d$. Prior to the measurement, the AFM cantilevers and substrates were cleaned using O_2 plasma generated in a Diener Zepto plasma system (process conditions: radio frequency power = 100 W, pressure = 300 mTorr, O_2 flow rate = 16.5 sccm, and duration = 3 min).

Surface Force Apparatus. An SFA-2000 apparatus (SurForce LLC, Santa Barbara, USA) was used to simultaneously measure distances and forces between molecularly smooth mica films in aqueous solutions. Mica films were cut from the same exfoliated "mother film" to ensure that they had equal thickness. These films were coated with a 50 nm-thick Au layer on one side. Each Au-coated mica film was then glued onto a transparent silica disc with a cylindrical radius of curvature, R, of 1−2 cm. Note: the Au-coated side was glued to the disc such that the pristine mica surface was exposed to the air (or an aqueous electrolyte) inside the SFA box. Pairs of mica/Au/glue/disk samples, were placed in a cross-cylinder geometry in the SFA box. The translucent gold layers facilitated a leaky optical cavity; the distance between these mirrors was measured via fringes of equal chromatic order (FECO) produced when white light passed through this interferometer.[38] Surfaces were first brought into contact in a dry N_2 environment to assess the films' thickness; the surfaces were then separated and approximately 50 μL of an aqueous solution was placed between the samples. The top surface remained fixed, and the bottom surface affixed to a cantilever was driven upward at ∼10 nm/s using a motor. Repulsion between the surfaces reduced the approach speed, which bent the cantilever ($k \approx 2$ kN/m); this bending force was recorded to characterize the surface forces.

RESULTS AND DISCUSSION

Single-crystal SiO_2/Si wafers and freshly cleaved muscovite mica surfaces are ultrasmooth and acquire a negative charge in aqueous solutions depending on the pH/pK_a relationships because of the deprotonation of Si−OH groups[39] and the leaching of K^+ ions,[20] respectively. These materials therefore serve as rigid substrates for comparing the behaviors of ions and zwitterions at electrified interfaces. Glycine was used as a surrogate osmolyte because it is a common amino acid with the

https://doi.org/10.1021/acs.jpcb.1c10388
J. Phys. Chem. B 2022, 126, 1852−1860

smallest hydrophobic unit. In the pH range 3−9, the majority of glycine molecules in water exist in the zwitterionic form; below and above this range, they display net positive and negative charges because of the $-NH_3^+$ and $-COO^-$ groups, respectively.[40] We next used AFM to measure the electrostatic force at the silica−silica interfaces and to probe glycine adsorption onto the electrified mica−water interface. Although colloidal probes were used in the former experiments, nanoscale tips were used in the latter experiments (Figure 1A and

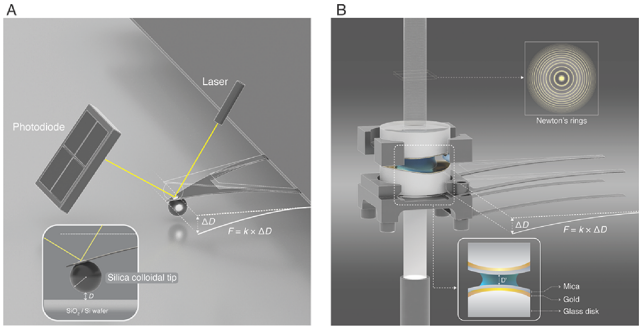

Figure 1. (A) Schematics of the AFM experiments. The relative distance between the AFM cantilever and the surface is determined by the displacement of the laser in the photodiode. The force is then measured on the basis of Hooke's law by detecting the deflection of the cantilever by the prevailing force between the AFM cantilever tip and the surface. The inset shows the contact geometry between a silica colloidal tip and a silica surface. (B) Schematics of the SFA. The absolute distance between two surfaces is calculated by interpreting the FECO. The force is then measured on the basis of Hooke's law by considering the difference between the calculated distance and the normal distance (without spring deflection) (image credits: Heno Hwang, Scientific Illustrator, KAUST).

Methods). In addition, we used SFA to achieve angstrom-scale resolution between ultrasmooth surfaces while measuring forces and pinpoint electrostatic decay lengths in various solutions.[38] Notably, although the contact area in the colloidal probe experiments was <300 nm^2, that in the SFA experiments was ∼100 μm^2 (Figure 1B and Methods). Results from these complementary techniques are presented in the following subsections.

Effects of Glycine Activity and Water pH on Electrostatic Forces between Surfaces. We conducted AFM experiments (for silica surfaces) and SFA experiments (for mica surfaces) using aqueous solutions of glycine in the concentration range 0.3−30 mM (pH ≈ 6.5) and pure water (pH ≈ 5.7) for comparison. Even though the zwitterionic concentration increased more than 100-fold, no differences were detected in the magnitude of the electrostatic forces and the Debye length in the silica−silica system (Figure 2A) and the mica−mica system in water (Figure 2B). That is, the addition of zwitterions did not affect the electrostatics in these systems; the electrostatics was similar to those in pure water. However, when we added hard ions i.e., KCl (0.01−10 mM) to 3 mM glycine solutions, the force magnitude decreased and the Debye lengths decreased from 45 nm at 0.01 mM to 29 nm at 0.1 mM, 10 nm at 1 mM, and 3 nm at 10 mM. These changes can be explained on the basis of the linearized Poisson−Boltzmann model (discussed later).

Next, we investigated the effects of the pH of 3 mM glycine solutions in the range 2−12 on surface forces for the silica−silica system (Figure 2C) and the mica−mica system (Figure 2D). The experimental results revealed that when 5 < pH < 7, the Debye length did not change (45 ± 7 nm); however, when pH < 5 or pH > 7, the Debye length decreased systematically as follows: from 29 nm at pH 4.4 to 3 nm at pH 2.1 and from 15 nm at pH 9.8 to 4 nm at pH 11.8. Later, we explain these observations based on the linearized Poisson−Boltzmann model and the speciation of glycine (into zwitterions and ions).

Adsorption of Glycine at an Electrified Interface as a Function of Water pH. We first incubated freshly cleaved mica surfaces in 30 mM glycine solutions at pH values of 1.7, 6.8, and 11.8 for 30 min to achieve chemical equilibrium. We then rinsed the surfaces with DI water, dried them with flowing N_2 gas, and imaged them by AFM (Figure 3A−C). We found that glycine self-assembled on mica only at pH 6.8, forming a patchy layer (Figure 3B); no adsorption occurred at pH values of 1.7 and 11.8 (Figure 3A,C). These results underscore the effects of the form of glycine (i.e., zwitterionic at pH 6.8 and ionic at other pH values) on its adsorption behavior (discussed later).

Electrical Conductivity, Osmotic Pressure, and Dielectric Constant of Glycine Solutions. We measured the ionic (or electrical) conductivities of glycine solutions as a function of their concentration and solution pH. At pH 7 ± 0.25, the ionic conductivities for 0.3, 3, and 30 mM glycine solutions were in the range 30−50 μS/cm (Figure 4A) and were independent of the solute concentration. In stark contrast, ionic conductivities of 3 mM glycine solutions increased to 250 μS/cm when the solution pH was adjusted to 3 or 9 (Figure 4B). Specifics of the differences between the anionic and cationic forms are discussed later.

We next quantified the osmolality of aqueous solutions as a function of the glycine concentration, added KCl content, and the pH. The experimental osmolality of the 0.3, 3, and 30 mM glycine solutions was 8.3 ± 1.7, 10.0 ± 0.1, and 33.5 ± 4.8 mOsmol/kg, respectively (Figure 4C). Similar trends were observed for the glycine solutions with different KCl concentrations; that is, osmolality increased with increasing KCl concentration. In addition, the measured osmolality of the 3 mM glycine solution with a pH in the range 4.4−9.6 was <12 mOsmol/kg, whereas at pH < 4.4 and pH > 9.6, the osmolality of the solution was >12 mOsmol/kg.

Lastly, we measured the dielectric constants of our glycine solutions as a function of their concentrations, added KCl content, and pH at 294 K (Figure 4D). The results show that the dielectric constants of (i) 0.3−30 mM glycine solutions, (ii) 3 mM glycine solutions containing 0.01−10 mM KCl, and (iii) 3 mM glycine solutions at pH 3.2−11.8 varied within 77.5 ± 0.3 to 79.2 ± 0.5, that is, within ±1% of the dielectric constant of pure water at 294 K and hence not significant. Curiously, the dielectric constant at pH 1.9 was comparatively lower, with a value of 75.6 ± 0.3.

Now, we draw upon our results to address the questions posed in the Introduction. Our key finding is that in dilute solutions, zwitterions layer/adsorb at electrified interfaces but do not electrostatically screen them. We explain why the addition of glycine leads to no observable differences in the Debye lengths and surface forces in the concentration range 0.3−30 mM, unlike the case where hard ions are present (Figure 2A,B).

To facilitate discussion, we first consider some important formulae related to the range and magnitude of electrostatic surface forces. The first equation is for the Debye length, $\lambda = \left(\frac{2N_A e^2 I}{\varepsilon_o \varepsilon_r k_B T}\right)^{-1/2}$, where $\varepsilon_o\varepsilon_r$ is the permittivity of the medium,

https://doi.org/10.1021/acs.jpcb.1c10388
J. Phys. Chem. B 2022, 126, 1852−1860

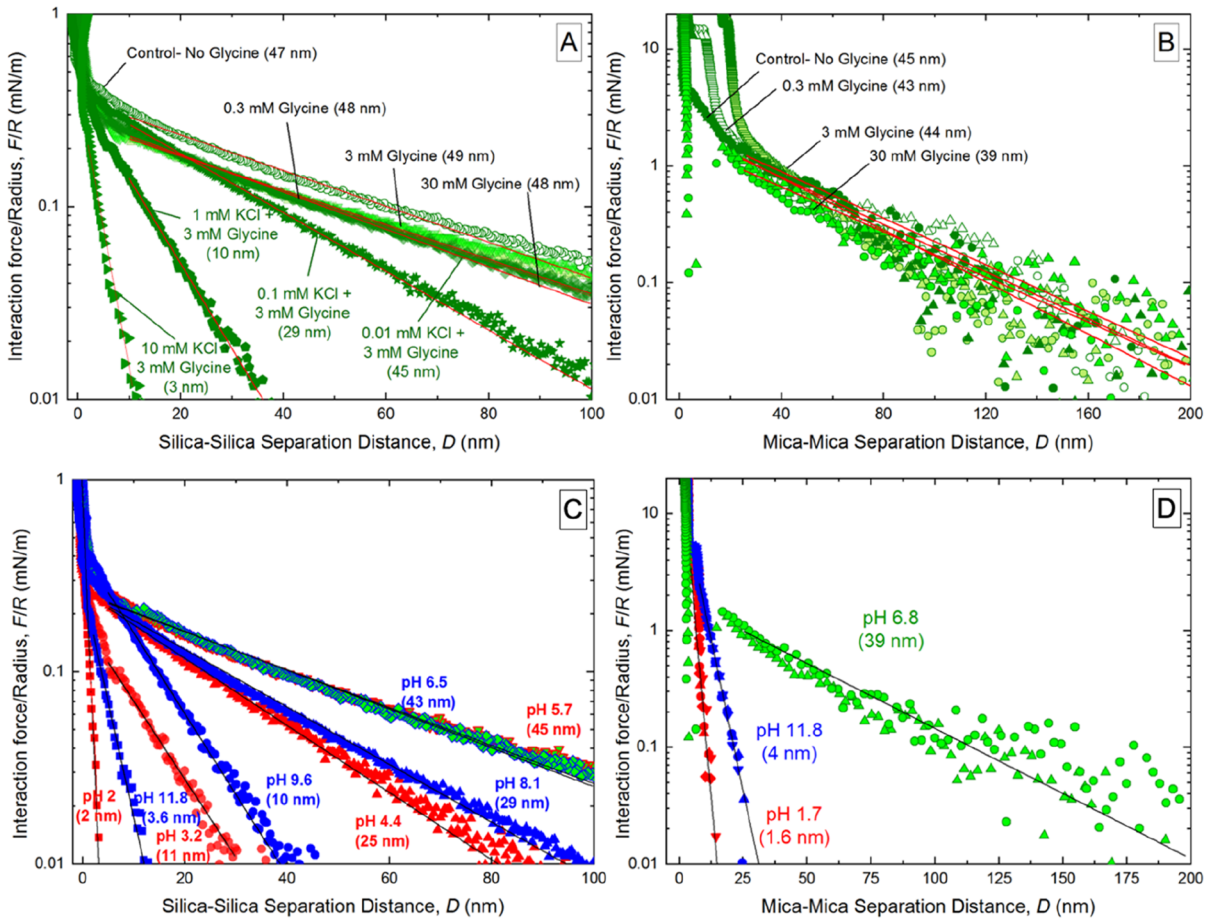

Figure 2. (A,B) Effects of the zwitterionic glycine concentration (0.3−30 mM; pH ≈ 6.5) on the electrostatic forces between charged surfaces in water with/without KCl. Semilogarithmic (A) AFM force data normalized by tip radius (for silica surfaces) and (B) SFA force data normalized by the effective radius of curvature of the discs (for mica surfaces). (C,D) Normalized force as a function of the surface separation at different pH values in 3 mM glycine solutions, as measured (C) between silica surfaces by AFM and (D) between mica surfaces by SFA. Under acidic conditions, the zwitterions and positively charged ions formed because protonation of the amine group dominated the chemical speciation of glycine. Under basic conditions, the zwitterions and negatively charged ions formed because deprotonation of the carboxylic group dominated the chemical speciation of glycine. The continuous lines are linear fits whose slope yields the Debye length, λ, which is listed within parentheses.

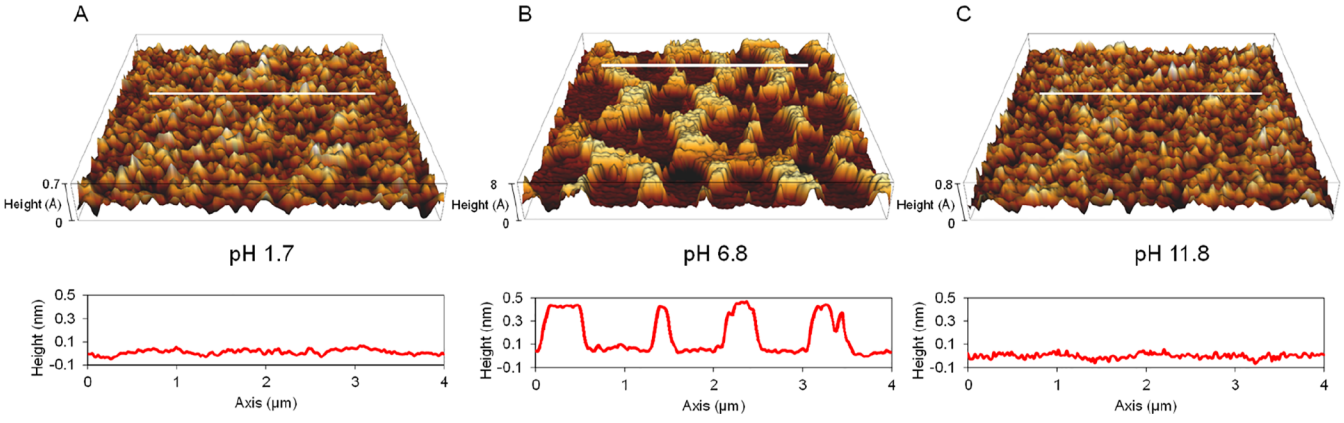

Figure 3. Three-dimensional AFM images of incubated mica in 30 mM glycine solution at different pH levels. Each image size is 5 × 5 μm^2. (A) Mica surface after incubation in 30 mM glycine solution at pH 1.7. The asperities' height is less than 0.7 Å. (C) Mica surface after incubation in 30 mM glycine solution at pH 6.8. The asperities' height is 4 Å. (C) Mica surface after incubation in 30 mM glycine solution at pH 11.8. The asperities' height is less than 0.8 Å.

N_A is Avogadro's number, e is the electronic charge, I is the ionic strength of the electrolytes, k_B is the Boltzmann constant, and T is the absolute temperature.[36] Ionic strength, in turn, is described by the equation $I = \frac{1}{2}\sum_i C_i z_i^2$, where C_i and z_i denote the concentration and charge of species i, respectively. Next, the expression for the normalized surface force investigated in our experiments can be analytically derived as

https://doi.org/10.1021/acs.jpcb.1c10388
J. Phys. Chem. B 2022, 126, 1852−1860

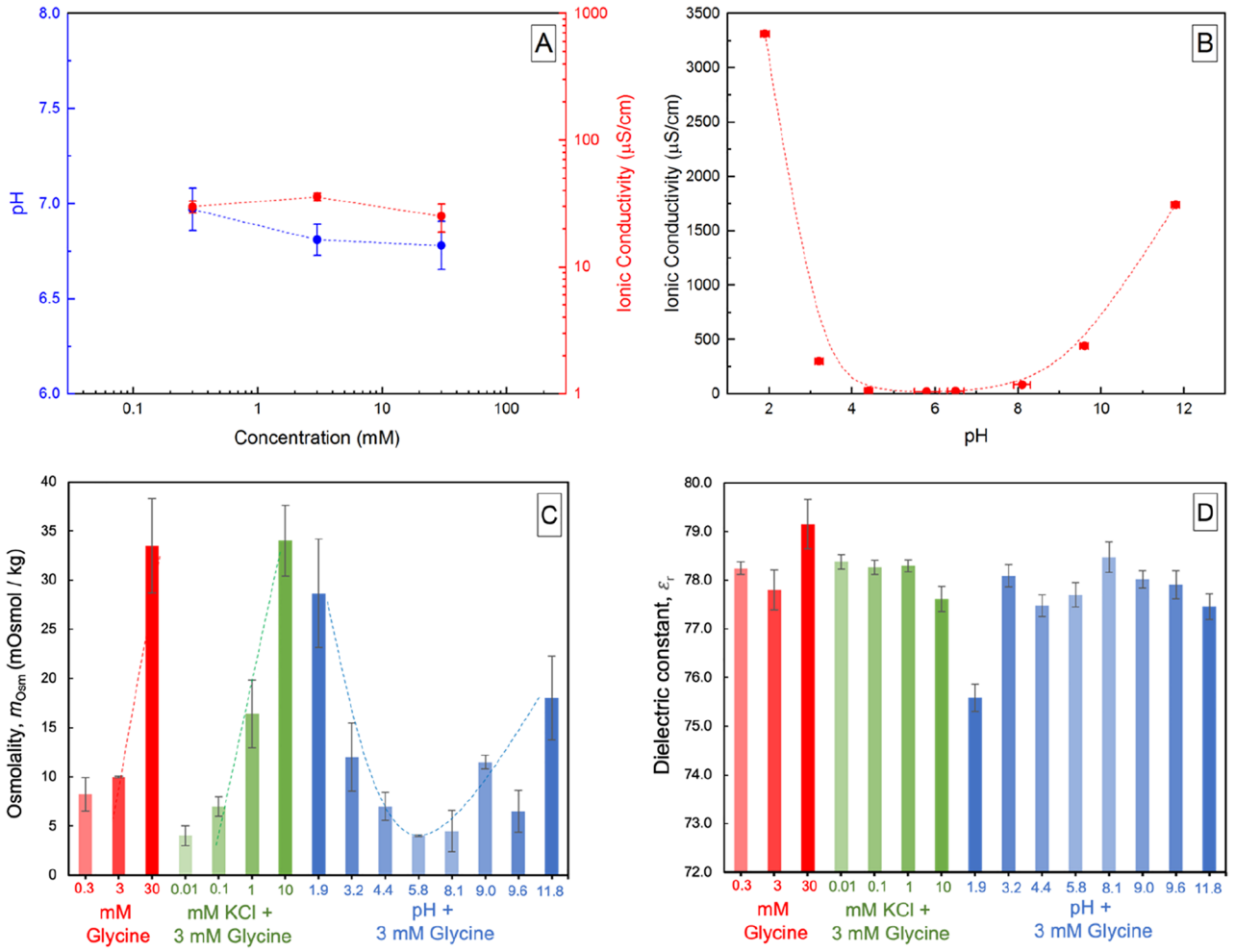

Figure 4. (A) Correlations between glycine concentration in water and the solution ionic conductivity (red) and pH (blue). (B) Effects of the solution pH on the ionic conductivities of 3 mM glycine solutions. Osmolality (C) and dielectric constants (D) of glycine solutions as a function of glycine concentration, addition of varying KCl concentrations, and solution pH. (Note: dotted lines/curves in the panels A−C are intended to serve as visual aid only).

$\frac{F}{R} = \left\{\frac{64\pi\varepsilon_o\varepsilon_r}{\lambda}\left(\frac{k_BT}{e}\right)^2 \tan h^2\left(\frac{e\psi_o}{4k_BT}\right)\right\}e^{-D/\lambda}$, where D is the separation distance between two surfaces and ψ_o is the surface potential.[20]

We now consider the dependence of λ on ε_r and I. The negligible variations in the measured surface forces' magnitude and range (Figure 2A,B) and the dielectric constants of glycine solutions, ε_r, in the range 0.3−30 mM (Figure 4D) imply that the contribution to I must also be minimal. This argument demonstrates that zwitterions do not contribute to I, and hence λ, in dilute solutions. This result challenges previous proposals for assigning partial/elementary charges[32,41−43] to zwitterions when estimating their contributions to I. Interestingly, the variation in the dielectric constants of 3 mM glycine solutions containing 0.01−10 mM KCl and whose pH values were adjusted in the range 3.2−11.8 is also small. We consider that in the pH range 4−9, the contributions of hard ions K^+, H^+, Cl^-, and OH^- and zwitterions are opposite: hard ions decrease the dielectric constant, whereas glycine increases it as $\varepsilon_r = 78.5 + \delta \times C_{osmolyte}$ [M], where δ = 22.6/mol.[44] At pH 1.9, the dielectric constant changes substantially, whereas this change is not observed at pH 11.8; this finding warrants further investigation.

Next, we use theory to pinpoint the effects of glycine's zwitterionic and ionic forms on the screening of the electrostatic potential of silica and mica surfaces. To this end, we conducted 100 force runs in each solution and analyzed the results statistically. Each curve was fitted with an exponential decay function, and pre-exponential factors in the linear (semi-logarithmic force−distance) regime were used to calculate surface potentials at the outer Helmholtz layer.[20] The calculated surface potentials for silica in 0.3, 3, and 30 mM glycine solutions were 42 ± 7 mV (Table 1). By contrast, the addition of 0.01, 0.1, 1, and 10 mM KCl to 3 mM glycine resulted in a dramatic decrease in the calculated surface potential from 40 to 38 mV, 25, and 10 mV, respectively. Together, these results demonstrate that zwitterions do not lead to electrostatic screening under dilute conditions. In addition, we repeated these experiments using AFM colloidal probes of different sizes and observed consistent trends (Supporting Information Figure S1).

Next, we explain the effects of water pH on the Debye lengths and surface forces in glycine solutions, as observed in our experiments with silica−silica (Figure 2A) and mica−mica systems (Figure 2B). In the pH range 7.8−11.8, glycine is present in the anionic state because of deprotonation of its $-NH_3^+$ and −COOH groups (Supporting Information Figures S2 and S3); in the pH < 5 range, glycine becomes a cation

https://doi.org/10.1021/acs.jpcb.1c10388
J. Phys. Chem. B 2022, 126, 1852−1860

Table 1. Summary of Experimental Data and Calculated Values Presented in the Present Work

pH	composition	ionic conductivity (μS/cm)	I (M)[a]	ε_r	m_{osm} (mOsmol/kg)	λ (nm)[b]	F/R (mN/m)[c]	Ψ_{silica} (mV)[b]
6.9 ± 0.3	0.3 mM glycine	29.8 ± 3.2	6.1×10^{-6}	78.2 ± 0.1	8.3 ± 1.7	46.1 ± 1.3	0.187	−40.7 ± 3.8
6.8 ± 0.3	3 mM glycine	35.7 ± 2.4	4.8×10^{-6}	77.8 ± 0.4	10.0 ± 0.1	45.7 ± 7.1	0.188	−41.5 ± 5.0
6.7 ± 0.2	30 mM glycine	25.1 ± 6.2	3.5×10^{-6}	79.2 ± 0.5	33.5 ± 4.8	48.1 ± 3.6	0.186	−43.4 ± 5.8
6.4 ± 0.3	3 mM glycine + 0.01 mM KCl	32.4 ± 1.1	7.4×10^{-6}	78.4 ± 0.1	34.0 ± 3.6	43.3 ± 1.6	0.188	−40.4 ± 6.1
6.2 ± 0.2	3 mM glycine + 0.1 mM KCl	96.3 ± 4.4	5.2×10^{-5}	78.3 ± 0.2	16.4 ± 3.4	27.6 ± 4.1	0.185	−38.6 ± 7.3
6.2 ± 0.2	3 mM glycine + 1 mM KCl	271.0 ± 0.5	5.0×10^{-4}	78.3 ± 0.1	7.0 ± 1.0	10.1 ± 0.9	0.05	−23.5 ± 8.3
6.2 ± 0.2	3 mM glycine +10 mM KCl	1461.8 ± 7.9	5.0×10^{-3}	77.6 ± 0.3	4.0 ± 1.0	4.5 ± 0.9	∼0	−9.6 ± 5.6
1.9 ± 0.1	3 mM glycine	3313.1 ± 5.86	1.5×10^{-2}	75.6 ± 0.3	28.7 ± 5.5	1.5 ± 0.5	∼0	−4.33 ± 0.6
3.2 ± 0.1	3 mM glycine	302.4 ± 4.40	1.0×10^{-3}	78.1 ± 0.2	12.0 ± 3.5	10.7 ± 0.9	0.03	−14.9 ± 4.8
4.4 ± 0.1	3 mM glycine	26.9 ± 5.49	6.6×10^{-5}	77.5 ± 0.2	7.0 ± 1.4	25.6 ± 0.4	0.11	−28.4 ± 3.1
5.8 ± 0.2	3 mM glycine	21.8 ± 17.16	2.6×10^{-6}	77.7 ± 0.2	4.0 ± 0.1	45.0 ± 2.3	0.17	−41.3 ± 4.9
6.5 ± 0.3	3 mM glycine	23.4 ± 15.37	2.4×10^{-6}	78.5 ± 0.3	4.5 ± 2.1	43.0 ± 1.6	0.17	−39.8 ± 4.8
8.1 ± 0.2	3 mM glycine	82.9 ± 7.02	9.3×10^{-5}	78.0 ± 0.3	11.5 ± 2.1	27.3 ± 2.0	0.13	−43.3 ± 4.9
9.6 ± 0.2	3 mM glycine	439.5 ± 8.96	1.5×10^{-3}	77.9 ± 0.3	6.5 ± 2.1	11.0 ± 0.9	0.06	−23.1 ± 9.3
11.8 ± 0.1	3 mM glycine	1740.5 ± 14.88	9.3×10^{-3}	77.5 ± 0.3	18.0 ± 4.2	3.6 ± 0.6	∼0	−6.9 ± 1.5

[a]Zwitterions do not contribute to ionic strength. [b]Average values from 100 force curves. [c]Magnitude of surface forces at 20 nm.

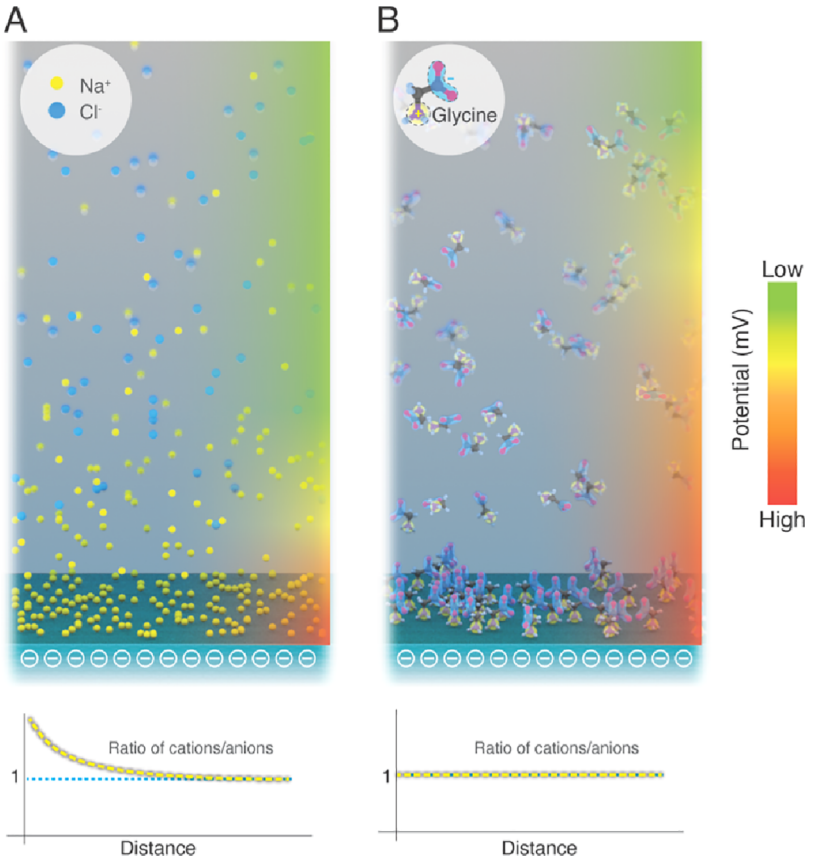

Figure 5. Schematic of the ion/molecule distribution on the negatively charged surface in an aqueous solution. (A) Illustration of monovalent ions on the negatively charged surface in an aqueous solution. The inset shows the concentration of monovalent cations and anions as a function of the distance from a negatively charged surface. (B) Illustration of zwitterions on the negatively charged surface in an aqueous solution. The inset illustrates the concentration of cations and anions on a zwitterionic osmolyte as a function of the distance from a negatively charged surface.

because of protonation of its $-NH_3$ and $-COO^-$ groups.[40] In its anionic and cationic states, glycine contributes to I, which influences λ and leads to a decrease in the magnitude and range of surface forces. By contrast, when the pH is in the range 4−9, glycine exists as a zwitterion and does not contribute to I, as previously demonstrated; thus, the Debye lengths are unaffected. In addition, the electrical conductivities of solutions containing purely ionic forms of glycine exhibit a conductivity as much as sixfold higher than that of solutions containing the zwitterionic form of glycine. Notably, water's intrinsic ionic strength cannot be neglected in solutions containing purely zwitterionic glycine. Table 1 summarizes the effects of the glycine concentration, added KCl content, and water pH on the electrical conductivity, I, ε_r, m_{osm}, λ, repulsive electrostatic forces (at 20 nm), and Ψ_{silica} at various pH values.

https://doi.org/10.1021/acs.jpcb.1c10388
J. Phys. Chem. B 2022, 126, 1852−1860

We here discuss our mechanistic understanding of the observed similarities and differences in the effects of zwitterions and ions at electrified interfaces. Textbook physics tells us that electrified interfaces repel similarly charged ions and attract counterions to form a diffuse electrical double layer (EDL). Consequently, the surface potential (or electrical charge density) perceived outside the EDL is substantially reduced (Figure 5A). Although zwitterions adsorb onto electrified interfaces (Figure 3B), they do not affect the net electrical potential (or the surface charge density) because each zwitterionic species comprises an explicit positive and negative charge (Figure 5B). This inseparability of the + and − charges precludes the accumulation of counterions, thereby obviating screening of electrical field/potential/charge density. Depending on the surface charge, adsorbed zwitterions might orient/distribute in a ± or ∓ alignment with the surface; depending on the surface charge density, a lateral interdigitation, ±∓±∓±∓, might also be possible along the surface. Nanoscale confinement between charged surfaces of similar/dissimilar surface charge density and ion polarization[45] could further complicate this matter. Curiously, when the solution pH is 11.8 (Figure 3C) and glycine transitions to its anionic form and it is repelled by the negatively charged surfaces, the cationic form (pH 1.7) (Figure 3A) also fails to adsorb onto the negatively charged surface; it is outcompeted by protons because their small size enables them to better fit into the negatively charged sites.[46] At electrified interfaces, zwitterions form a layer akin to the Helmholtz layer of hard ions; however, their distribution might not follow Boltzmann statistics. However, our experimental results cannot provide quantitative insight into the competition between the simple cations and the $-NH_3^+$ group of the zwitterions for the negatively charged sites on silica surfaces; these aspects should be probed via complementary computational simulations.

Lastly, we comment on the contribution of glycine speciation on surface forces in concentrated solutions. We remind the reader that in the pH range 5−7, more than 99.95% of glycine remains in the zwitterion state (Supporting Information Figure S3). Thus, in dilute solutions (e.g., ≲30 mM), the ionic form of glycine is only 0.05% and its contribution to the ionic strength is 1.5×10^{-6} M. This contribution is, in fact, lower than the ionic strength of water in equilibrium with atmospheric CO_2 (pH 5.6, 5×10^{-6} M). Therefore, the effects of speciation are negligible in dilute glycine solutions. By contrast, if the glycine concentration is very high, for example, 3 M in the pH range 5−7, the speciation into the ionic form would be ∼15 mM, which is expected to suppress electrostatics with a Debye length of 2−3 nm. Therefore, our results are consistent with the latest findings on the resurrection of electrostatics at high (1−3 M) osmolyte concentrations. It is also interesting to note that even though zwitterions do not affect ionic strength, surface forces, potentials, or Debye lengths, they do contribute to solutions' osmotic pressure (Figure 4C). The van't Hoff equation describes this relationship as $\Pi = RT\sum_i n_i C_i$, where Π is the osmotic pressure, R is the universal gas constant, T is the absolute temperature, and n_i is the van't Hoff factor. Note that the observed nonlinearity in the osmolality measurements at 0.3 mM is attributed to the instrument's limited accuracy outside its operating range (20−3200 mOsmol/kg).

CONCLUSIONS

Our curiosity-driven investigation of zwitterions and ions at electrified surfaces revealed that zwitterions can orchestrate a significantly broader range of effects than hard ions tuned via their concentration and the solution pH. Whereas hard ions such as K^+ and Cl^- always contribute to ionic strength in dilute solutions, zwitterions do not. While hard ions adsorb at charged interfaces and screen them, zwitterions form a layer at charged interfaces but do not screen them. Therefore, the magnitudes and ranges of electrostatic surface forces remain unaffected in zwitterionic solutions. These distinctive behaviors of zwitterions are due to their unusual structure that renders the positive and negative charges inseparable. Thus, zwitterions do not impact electrostatics inside the EDL and the Boltzmann distribution is consequently not relevant to describe their interfacial activity. Zwitterionic surface adsorption would likely depend on the interfacial charge density, the molecular dimensions of zwitterions, and competing effects with other species, for example, protons; molecular simulations are warranted to probe this further. Our surface force measurements demonstrate how zwitterions, but not hard ions, can maintain the finely tuned balance of electrostatic forces, Debye lengths, and electrical conductivities in dilute solutions with concentrations varying more than 100-fold. Simultaneously, zwitterions contribute to the osmotic pressure in the same manner as hard ions. Therefore, they can facilitate a reliable evolutionary strategy to support life under osmotic stresses. Our report thus provides a surface force-based reductionist rationale for the exploitation of zwitterionic osmolytes such as glycine by extremophiles. These findings should also guide the rational design of biocatalysts,[47] energy harvesting,[48] nanofluidic devices,[49,50] and beyond.[26]

ASSOCIATED CONTENT

Supporting Information

The Supporting Information is available free of charge at https://pubs.acs.org/doi/10.1021/acs.jpcb.1c10388.

Effects of glycine on the screening lengths and the normalized force−distance curves for the silica−silica system probed via AFM using colloidal probes of radius 6.6 μm; chemical speciation of glycine as a function of solution pH; and fractions of different states of the amino acid glycine at different pH values (PDF)

AUTHOR INFORMATION

Corresponding Author

Himanshu Mishra − *Environmental Science and Engineering (EnSE) Program, Biological and Environmental Science and Engineering (BESE) Division and Interfacial Lab (iLab), Water Desalination and Reuse Center (WDRC), King Abdullah University of Science and Technology (KAUST), Thuwal 23955-6900, Saudi Arabia;* orcid.org/0000-0001-8759-7812; Email: himanshu.mishra@kaust.edu.sa

Authors

Muhammad Ghifari Ridwan − *Environmental Science and Engineering (EnSE) Program, Biological and Environmental Science and Engineering (BESE) Division and Interfacial Lab (iLab), Water Desalination and Reuse Center (WDRC), King Abdullah University of Science and Technology (KAUST), Thuwal 23955-6900, Saudi Arabia*

Buddha Ratna Shrestha − *Environmental Science and Engineering (EnSE) Program, Biological and Environmental Science and Engineering (BESE) Division and Interfacial Lab (iLab), Water Desalination and Reuse Center (WDRC), King*

https://doi.org/10.1021/acs.jpcb.1c10388
J. Phys. Chem. B 2022, 126, 1852−1860

Abdullah University of Science and Technology (KAUST), Thuwal 23955-6900, Saudi Arabia

Nischal Maharjan − *Environmental Science and Engineering (EnSE) Program, Biological and Environmental Science and Engineering (BESE) Division and Interfacial Lab (iLab), Water Desalination and Reuse Center (WDRC), King Abdullah University of Science and Technology (KAUST), Thuwal 23955-6900, Saudi Arabia*

Complete contact information is available at: https://pubs.acs.org/10.1021/acs.jpcb.1c10388

Author Contributions

H.M. conceived the project and supervised the research. M.G.R. and B.R.S. performed AFM and SFA experiments. N.M. performed electrical conductivity and pH measurements. M.G.R. and N.M. performed osmotic pressure measurements. M.G.R. analyzed the dielectric response data and the osmotic pressure data. H.M. and M.G.R. wrote the manuscript with assistance from B.R.S. and N.M.

Notes

The authors declare no competing financial interest.

Additional data of AFM measurement between silica surface and silica colloidal probe and glycine speciation.

Data Availability: The authors declare that all the data supporting the findings of this study are available within the paper and its Supporting Information. All data available in this work are available from the authors as per request.

■ ACKNOWLEDGMENTS

H.M. thanks Changzi Wang, a student from his course on Aquatic Chemistry (EnSE 202) at KAUST, for bringing this problem to his attention. The authors are indebted to Masha Belyi (Research Scientist, Amazon's Team Alexa) for creating a Python script for analyzing hundreds of AFM force−distance curves generated in this work to pinpoint the trends in Debye lengths and surface potentials. M.G.R. thanks Mohammad Abbas (KAUST) for discussions on cell physiology; B.R.S. thanks Dr. Bruno Torres (KAUST) for providing colloidal probes for AFM experiments. The co-authors thank Ana Rouseva (KAUST) and Paulus Buijs (KAUST) for assisting with osmotic pressure measurements presented in Figure 4C; Dr. Farizal Hakiki (KAUST) and Prof. Carlos Santamarina (KAUST) for characterizing dielectric responses of solutions presented in Figure 4D; and Heno Hwang, KAUST Illustrator, for preparing Figures 1and 5 and TOC. H.M. acknowledges KAUST for funding (grant no. BAS/1/1070-01-01).

■ REFERENCES

(1) Yancey, P. H.; Clark, M. E.; Hand, S. C.; Bowlus, R. D.; Somero, G. N. Living with water stress: evolution of osmolyte systems. *Science* **1982**, *217*, 1214.

(2) Warshel, A.; Sharma, P. K.; Kato, M.; Xiang, Y.; Liu, H.; Olsson, M. H. M. Electrostatic Basis for Enzyme Catalysis. *Chem. Rev.* **2006**, *106*, 3210−3235.

(3) Tanford, C.; Reynolds, J. *Nature's Robots: A History of Proteins*; Oxford University Press: New York, 2003.

(4) Mukherjee, M.; Mondal, J. Unifying the Contrasting Mechanisms of Protein-Stabilizing Osmolytes. *J. Phys. Chem. B* **2020**, *124*, 6565−6574.

(5) Mishra, H.; Enami, S.; Nielsen, R. J.; Hoffmann, M. R.; Goddard, W. A.; Colussi, A. J. Anions dramatically enhance proton transfer through aqueous interfaces. *Proc. Natl. Acad. Sci. U.S.A.* **2012**, *109*, 10228−10232.

(6) Mishra, H.; Nielsen, R. J.; Enami, S.; Hoffmann, M. R.; Colussi, A. J.; Goddard, W. A. Quantum chemical insights into the dissociation of nitric acid on the surface of aqueous electrolytes. *Int. J. Quantum Chem.* **2013**, *113*, 413−417.

(7) Colussi, A. J.; Enami, S.; Yabushita, A.; Hoffmann, M. R.; Liu, W.-G.; Mishra, H.; Goddard III, W. A., III Tropospheric aerosol as a reactive intermediate. *Faraday Discuss.* **2013**, *165*, 407−420.

(8) Hillel, D. *Introduction to Soil Physics*; Academic Press: New York, NY, 1982.

(9) Gallo, A., Jr; Musskopf, N. H.; Liu, X.; Yang, Z.; Petry, J.; Zhang, P.; Thoroddsen, S. T.; Im, H. G.; Mishra, H. On the Formation of Hydrogen Peroxide in Water Microdroplets. *Chem. Sci.* **2022**, DOI: 10.1039/D1SC06465G.

(10) Musskopf, N. H.; Gallo, A.; Zhang, P.; Petry, J.; Mishra, H. The Air-Water Interface of Water Microdroplets Formed by Ultrasonication or Condensation Does Not Produce H2O2. *J. Phys. Chem. Lett.* **2021**, *12*, 11422−11429.

(11) Enami, S.; Mishra, H.; Hoffmann, M. R.; Colussi, A. J. Protonation and Oligomerization of Gaseous Isoprene on Mildly Acidic Surfaces: Implications for Atmospheric Chemistry. *J. Phys. Chem. A* **2012**, *116*, 6027−6032.

(12) Carrouel, F.; Viennot, S.; Ottolenghi, L.; Gaillard, C.; Bourgeois, D. Nanoparticles as Anti-Microbial, Anti-Inflammatory, and Remineralizing Agents in Oral Care Cosmetics: A Review of the Current Situation. *Nanomaterials* **2020**, *10*, 140.

(13) Das, R.; Arunachalam, S.; Ahmad, Z.; Manalastas, E.; Mishra, H. Bio-inspired gas-entrapping membranes (GEMs) derived from common water-wet materials for green desalination. *J. Membr. Sci.* **2019**, *588*, 117185.

(14) Santana, A.; Farinha, A. S. F.; Toraño, A. Z.; Ibrahim, M.; Mishra, H. A first-principles approach for treating wastewaters. *Int. J. Quantum Chem.* **2021**, *121*, No. e26501.

(15) Nauruzbayeva, J.; Sun, Z.; Gallo, A.; Ibrahim, M.; Santamarina, J. C.; Mishra, H. Electrification at water−hydrophobe interfaces. *Nat. Commun.* **2020**, *11*, 5285.

(16) Benjamin, M. M., *Water Chemistry*. 2nd ed.; Waveland Press, Inc.: Long Grove, IL, USA, 2015.

(17) Dishon, M.; Zohar, O.; Sivan, U. From Repulsion to Attraction and Back to Repulsion: The Effect of NaCl, KCl, and CsCl on the Force between Silica Surfaces in Aqueous Solution. *Langmuir* **2009**, *25*, 2831−2836.

(18) Lee, A. A.; Perez-Martinez, C. S.; Smith, A. M.; Perkin, S. Scaling Analysis of the Screening Length in Concentrated Electrolytes. *Phys. Rev. Lett.* **2017**, *119*, 026002.

(19) Ma, C. D.; Wang, C.; Acevedo-Vélez, C.; Gellman, S. H.; Abbott, N. L. Modulation of hydrophobic interactions by proximally immobilized ions. *Nature* **2015**, *517*, 347−350.

(20) Israelachvili, J. N., *Intermolecular and Surface Forces*. 3rd ed.; Academic Press, Elsevier Inc.: 2011.

(21) Ravera, F.; Dziza, K.; Santini, E.; Cristofolini, L.; Liggieri, L. Emulsification and emulsion stability: The role of the interfacial properties. *Adv. Colloid Interface Sci.* **2021**, *288*, 102344.

(22) Hasegawa, P. M.; Bressan, R. A.; Zhu, J.-K.; Bohnert, H. J. Plant cellular and molecular responses to high salinity. *Annu. Rev. Plant Physiol. Plant Mol. Biol.* **2000**, *51*, 463−499.

(23) Famiglietti, J. S.; Ferguson, G. The hidden crisis beneath our feet. *Science* **2021**, *372*, 344.

(24) Coleridge, S. T. *The Rime of the Ancient Mariner*; Dover Publications, 1992.

(25) Yancey, P. H. Organic osmolytes as compatible, metabolic and counteracting cytoprotectants in high osmolarity and other stresses. *J. Exp. Biol.* **2005**, *208*, 2819.

(26) Rothschild, L. J.; Mancinelli, R. L. Life in extreme environments. *Nature* **2001**, *409*, 1092−1101.

(27) Abobatta, W. F. Plant Responses and Tolerance to Extreme Salinity: Learning from Halophyte Tolerance to Extreme Salinity. In *Salt and Drought Stress Tolerance in Plants: Signaling Networks and Adaptive Mechanisms*; Hasanuzzaman, M., Tanveer, M., Eds.; Springer

International Publishing: Cham, 2020, pp 177−210. DOI: 10.1007/978-3-030-40277-8_7
(28) Kamerlin, S. C. L.; Warshel, A. At the dawn of the 21st century: Is dynamics the missing link for understanding enzyme catalysis? *Proteins: Struct., Funct., Bioinf.* **2010**, *78*, 1339−1375.
(29) Shrestha, B. R.; Pillai, S.; Santana, A.; Donaldson Jr, S. H., Jr; Pascal, T. A.; Mishra, H. Nuclear Quantum Effects in Hydrophobic Nanoconfinement. *J. Phys. Chem. Lett.* **2019**, *10*, 5530−5535.
(30) Lang, F.; Busch, G. L.; Ritter, M.; Völkl, H.; Waldegger, S.; Gulbins, E.; Häussinger, D. Functional Significance of Cell Volume Regulatory Mechanisms. *Physiol. Rev.* **1998**, *78*, 247−306.
(31) Stellwagen, E.; Prantner, J. D.; Stellwagen, N. C. Do zwitterions contribute to the ionic strength of a solution? *Anal. Biochem.* **2008**, *373*, 407−409.
(32) Cecchi, T.; Pucciarelli, F.; Passamonti, P. Ion-interaction chromatography of zwitterions. The fractional charge approach to model the influence of the mobile phase concentration of the ion-interaction reagent. *Analyst* **2004**, *129*, 1037−1046.
(33) Kamerlin, S. C. L.; Sharma, P. K.; Chu, Z. T.; Warshel, A. Ketosteroid isomerase provides further support for the idea that enzymes work by electrostatic preorganization. *Proc. Natl. Acad. Sci. U.S.A.* **2010**, *107*, 4075.
(34) Israelachvili, J.; Wennerström, H. Role of hydration and water structure in biological and colloidal interactions. *Nature* **1996**, *379*, 219−225.
(35) Baimpos, T.; Shrestha, B. R.; Raman, S.; Valtiner, M. Effect of Interfacial Ion Structuring on Range and Magnitude of Electric Double Layer, Hydration, and Adhesive Interactions between Mica Surfaces in 0.05-3 M Li+ and Cs+ Electrolyte Solutions. *Langmuir* **2014**, *30*, 4322−4332.
(36) Govrin, R.; Tcherner, S.; Obstbaum, T.; Sivan, U. Zwitterionic Osmolytes Resurrect Electrostatic Interactions Screened by Salt. *J. Am. Chem. Soc.* **2018**, *140*, 14206−14210.
(37) Butt, H.-J.; Cappella, B.; Kappl, M. Force measurements with the atomic force microscope: Technique, interpretation and applications. *Surf. Sci. Rep.* **2005**, *59*, 1−152.
(38) Israelachvili, J.; Min, Y.; Akbulut, M.; Alig, A.; Carver, G.; Greene, W.; Kristiansen, K.; Meyer, E.; Pesika, N.; Rosenberg, K.; Zeng, H. Recent advances in the surface forces apparatus (SFA) technique. *Rep. Prog. Phys.* **2010**, *73*, 036601.
(39) Iler, R. K. *The colloid chemistry of silica and silicates*. LWW, 1955; Vol. *80*.
(40) McMurry, J. *Organic Chemistry*; Brooks/Cole: USA, 2000; Vol. *895*, p 1003.
(41) Wenner, J. R.; Bloomfield, V. A. Buffer Effects onEcoRV Kinetics as Measured by Fluorescent Staining and Digital Imaging of Plasmid Cleavage. *Anal. Biochem.* **1999**, *268*, 201−212.
(42) Karamanos, N. K.; Lamari, F. State-of-the-art of capillary electrophoresis with application to the area of glycoconjugates. *Biomed. Chromatogr.* **1999**, *13*, 501−506.
(43) Romanenko, V. G.; Rothblat, G. H.; Levitan, I. Sensitivity of Volume-regulated Anion Current to Cholesterol Structural Analogues. *J. Gen. Physiol.* **2003**, *123*, 77−88.
(44) Oster, G.; Price, D.; Joyner, L. G.; Kirkwood, J. G. The Dielectric Constants of Solutions of Glycine and Pyridine Betaine in Water-Dioxane Mixtures. *J. Am. Chem. Soc.* **1944**, *66*, 946−948.
(45) Jungwirth, P.; Tobias, D. J. Specific Ion Effects at the Air/Water Interface. *Chem. Rev.* **2006**, *106*, 1259−1281.
(46) Pashley, R. M.; Israelachvili, J. N. DLVO and hydration forces between mica surfaces in Mg^{2+}, Ca^{2+}, Sr^{2+}, and Ba^{2+} chloride solutions. *J. Colloid Interface Sci.* **1984**, *97*, 446−455.
(47) Gomes, J.; Steiner, W. The Biocatalytic Potential of Extremophiles and Extremozymes. *Food Technol. Biotechnol.* **2004**, *42*, 223−225.
(48) Xu, W.; Zheng, H.; Liu, Y.; Zhou, X.; Zhang, C.; Song, Y.; Deng, X.; Leung, M.; Yang, Z.; Xu, R. X.; Wang, Z. L.; Zeng, X. C.; Wang, Z. A droplet-based electricity generator with high instantaneous power density. *Nature* **2020**, *578*, 392−396.
(49) Bocquet, L. Nanofluidics coming of age. *Nat. Mater.* **2020**, *19*, 254−256.
(50) Robin, P.; Kavokine, N.; Bocquet, L. Modeling of emergent memory and voltage spiking in ionic transport through angstrom-scale slits. *Science* **2021**, *373*, 687.

https://doi.org/10.1021/acs.jpcb.1c10388
J. Phys. Chem. B 2022, 126, 1852−1860